Recueil De Mécanique
Centre Universitaire
El Wancharissi de Tissemsilt

Research Paper *DOI : 10.5281/zenodo.1169845* *Open access*

Characterization of thermally affected steels by nanoindentation

Caractérisation des aciers affectés thermiquement par nanoindentation

***Samir HABIBI*[a,b,*], *Noureddine MAHMOUDI*[b], *BenaoumeurAOUR*[c], *Laid AMINALLAH*[a], *Ould Chikh BAHRI*[a]**

[a]*Departement de Génie Mécanique, Université Mustapha Stambouli de Mascara, BP 305, 29000 Mascara, Algérie.*

[b]*Laboratoire Génie Industriel et Développement Durable,Centre Universitaire de Relizane, 48000 Relizane, Algérie.*

[c]*Laboratoire Biomécanique Appliquée et Biomatériaux, Ecole Nationale Polytechnique d'Oran, 31000 Oran, Algérie*

ARTICLE INFO

Article history:

Received 19 December 17

Received in revised form 15 January 18

Accepted 20 January 18

Keywords:

Heat treatments; Characterization; Nanoindentation; Modulus of elasticity; Hardness.

Mots clés:

Traitements thermiques; Caractérisation; Nanoindentation; Module d'élasticité; Dureté

ABSTRACT

The thermal affectation is the basis of metallurgical modifications of the base metal which can induce fragilities, decreases in mechanical strength, lack of ductility ... These modifications depend on the material examined, the process used, the mode of operation followed ... This research is devoted to the experimental study, whose objective is the study of low-carbon steels who sustained of the various heat treatments. Then, the instrumented nanoindentation test is developed to analyze the characteristic loading and unloading curves of the examined specimens. In this case, we focus on the effect of heat treatments on the metallographic examination and the mechanical properties of the studied steels. At the same time, we study the coherence of the results obtained between the heat treatment and the nanoindentation process in the determination of elasticity modulus and hardness.

RÉSUMÉ

L'affectation thermique est à la base des modifications métallurgiques du métal de base qui peuvent induire des fragilités, des diminutions de la résistance mécanique, un manque de ductilité ... Ces modifications dépendent du matériau examiné, du procédé utilisé, du mode de fonctionnement suivi ... La recherche est consacrée à l'étude expérimentale, dont l'objectif est l'étude des aciers à faible teneur en carbone qui ont subi les différents traitements thermiques. Ensuite, le test de nanoindentation instrumenté est développé pour analyser les courbes caractéristiques de chargement et de déchargement des spécimens examinés. Dans ce cas, nous nous intéressons à l'effet des traitements thermiques sur l'examen métallographique et aux propriétés mécaniques des aciers étudiés. En même temps, nous étudions la cohérence des résultats obtenus entre le traitement thermique et le processus de nanoindentation dans la détermination du module d'élasticité et de la dureté.

* *Corresponding author. Tel.: +213 71693309.*
E-mail address: habibismr@yahoo.com

1 Introduction

The mechanical characterization of materials remains today a major stake for their industrial development. This characterization requires a thorough knowledge of the indentation test commonly used to determine local mechanical properties [1] and in particular thermally affected materials, such as the thermally affected area, or materials that undergo heat transfer that are likely to affect given structure [2]. And, makes it possible to question the relevance of this new tool for the exploration of the examined materials [3].In nanoindentation, it becomes difficult, for reasons of scale [4-7], to reach directly the parameters expected [8]. This article is devoted to the study of the local mechanical properties of low carbon steels that have undergone thermal treatments by applying experimental tests of nanoindentation. This examination takes place through five respective objectives:

- The determination of the depth of contact, hc, and the contact area, Ac,
- Calculation of the HIT hardness, and of the modulus of elasticity, EIT,
- Estimate the contact stiffness, S,
- Estimation of the hardness scale factor values, and the density of the dislocations involved in the deformation process,
- Confrontation of the results of heat treatment with those of the nanoindentation process.

2 Specimens and experimental protocol

We used a nanoindenter that can operate at higher temperatures, from ambient to 900°C. The specimens used are two steels with low carbon contents. The specimens are debited from a bar which undergoes a first standardization treatment. Specimen No. 1: This heat treatment consists of heating the sample for a period of one hour at 850°C and then carrying out a sudden cooling by quenching with water. Then, an income is applied for a period of one hour at 150°C. Specimen No. 2: This last phase is devoted to subjecting this material to three cycles of temperature flux between 900°C and 600°C. Thereafter, the sample cools slowly.

Experimental indentation tests were performed [9] on low carbon steel films deposited on glass slides using an MCT instrumented Vickers nanoindentor (Instrument CSM2-107). For each sample, at least 22 trials were conducted with maximum loads ranging from 10mN to 10N. The load is applied at a speed of 40mN/min. The maximum load is maintained for 15s and then gradually withdrawn at a speed of 40mN/min. All force-penetration results curves were then exported and processed using Matlab software in order to calculate the mechanical properties of the materials studied. The measurements are estimated at 150 nm for the penetrator Vickers [10].

3 Theoretical

In its general principle, the instrumented indentation test can record the displacement of the indenter during the whole cycle of loading and unloading. Analysis of the unloading curve leads to a value of the contact depth that takes into account the actual contact between the indenter and the material. This methodology was developed by Oliver and Pharr [11].

3.1 Analysis of a Load-Displacement Curve

3.1.1 Determination of Contact Depth and the Rigidity of Contact

The instrumented indentation draws its sources from the definition of contact between two bodies. As regards, in particular, the indentation has been the object of investigation of several authors from a mechanical point of view. The instrumented indentation (or Depth Sensing Indentation- DSI) prevents the observation of the residual indentation impression, unlike the conventional method for the determination of the hardness. In an instrumented indentation test, the diamond point is pressed to the sample surface up to a maximum load value given as conventional indentation or to a specified depth. Whatever the method, simultaneously records the load and the displacement of the indenter as shown in Fig. 1. This figure is interesting because it shows in key locations the position of the indenter into the material.

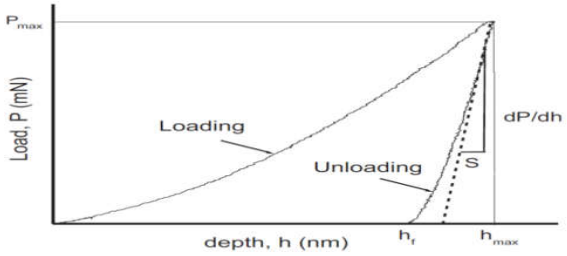

Fig. 1 Schematic representation of a load-displacement curve Obtained by a nanoindentation experiment and parameters needed for analysis [7]

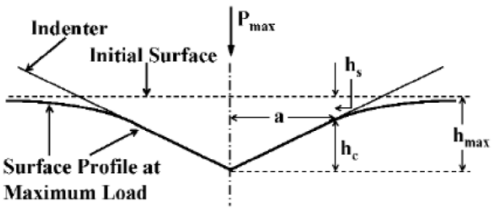

Fig. 2 Representation of the geometry of maximum indentation load for an ideal conical indenter [12]

In this figure, there representations h_{max} which corresponds to the maximum depth reached, h_f is the residual depth after removal of the indenter, h_R of which is determined by the slope of the unloading curve (it is noted h_c for ε = 1 in Fig. 1) and hc which the contact depth is used in the calculation of the hardness of Oliver and Pharr [11], which is offset from the h_R depth by an amount which depends on the parameter ε. This depth is derived from the value of h_R. Fig. 2 to better see the different sizes determined by instrumented indentation. The method of Oliver and Pharr relies on the expression used to represent the variation of the load as a function of depth in the unloading part of the curve:

$$P= B.(h-h_f)^m \quad (1)$$

Where P is the applied load, h recorded depth, h_f is determined after the complete withdrawal of the indenter, h_s is the difference between h_{max} and h_c. B and m are coefficients which depend on the nature of the material. In a recent work, Chicot et al. [9] suggest the rank between 40-89% of the maximum load P_{max}, for a better quality of smoothing.

As shown in Fig. 1, the calculation of h_R (h_c for ε = 1) is obtained by intersection of the tangent to the curve at discharge (generally called contact stiffness and denoted S) calculated in the maximum applied load P_{max}, with the x-axis, namely:

$$h_R=h_{max}-\frac{P_{max}}{S_u} \quad (2)$$

Where S_u is the slope of the unloading curve calculated for h equal to h_{max}. This slope is obtained by differentiating equation (1):

$$S_u= \left(\frac{dP}{dh}\right)_{h=hmax}= m.B.(h_{max}-h_f)^{m-1} \quad (3)$$

The relationship that can calculate the depth of the contact, h_c, is similar to the equation (2) which has been introduced in a pure ε parameter to consider the deformation of the fingerprint (deflection of -Sink-in faces). This relationship is as follows:

$$h_c=h_{max}-\varepsilon.\frac{P_{max}}{S_u} \quad (4)$$

Where ε value depend ofindenter type's. However, when observing the deformations around the print due to a material of reflux (pile-up), this equation is no longer applicable. Finally, the value of ε depends on the parameter m exponent value of the power law [13]. The theoretical values of m and ε parameters depending on the geometry of the contact, for the three most common forms [14], where m is the exponent of the power law and ε is the factor used in determining the depth of Contact. However, the value of ε corresponding to 0.75 m = 1.5 is almost always used for spherical indenter, cone and pyramid.

3.1.2 The contact area

As we mentioned in the definition of hardness, there involves a contact area between the indenter and the material. A_s in the case of the conventional hardness, one can use a projected area which is observed on the surface of the sample or the actual contact area which takes into account the surface of the inclined faces of the impression. The projected contact area Ac, is a key factor for the calculation of mechanical parameters. For perfect indenter geometry, Berkovich indenter pyramid with three faces, Vickers pyramid indenter and four-sided, the projected contact surface is proportional to the square of the contact depth hc as indicated by the following expression:

$$A = 24.56\ h_c^2 \tag{5}$$

3.2 Determination of Mechanical Properties

The indentation allows testing from the latest experimental techniques to obtain two mechanical properties among the most important, namely the hardness and elastic modulus of the material.

3.2.1 Hardness

Hardness is defined as the mechanical strength the material opposes the penetration of the indentor. The number of the hardness test is deduced is obtained from the ratio of the indentation load applied by a representative area of the imprint. The most general form is as follows:

$$H = \frac{P}{A} \tag{6}$$

Where P is the load and A is a representative area of the imprint. It is possible to calculate the hardness from the method of calculating the depth of contact. According to the definition of hardness, it is possible to propose hardness calculations that take into account the maximum depth reached, the residual depth, or to the contact depth knowledge that can be considered in each case either the projected area or the actual contact area.

3.2.2 Young's modulus

Determining the modulus of elasticity is based on the analysis of the unloading curve for the removal of the indenter is conditioned by the springback due to the elasticity of the material. It is again the slope from the determination of the modulus of elasticity will be. The method is based on the Hertz theory [14] recovery by Bulychec [15] and then developed by Sneddon [16]. It provides that the slope at the beginning of discharge can be written as a function of the contact area and the reduced modulus in the form:

$$S_u = \left(\frac{dP}{dh}\right)_{h=hmax} = \frac{2}{\sqrt{\pi}} E_R \sqrt{A_{cp}} \tag{7}$$

Where S_u is the stiffness of the contact between the indenter and the material during unloading, measured at maximum penetration, h_{max}. A_{cp} is the projected contact area and E_R is the reduced modulus of elasticity. The reduced modulus takes into account the elastic properties of the indenter, so the diamond or chromium carbide as appropriate. The relationship which gives the reduced module which allows obtaining the elastic modulus of the material is:

$$\frac{1}{E_R} = \frac{(1-\nu_m^2)}{E_m} + \frac{(1-\nu_i^2)}{E_i} \tag{8}$$

Where E and ν are the modulus of elasticity and the coefficient of fish, and the indices i and m refer to the characteristics of the indenter and the material. Under these conditions, the elastic modulus of the material is derived from the relationships (7) and (8) as follows:

$$E_m = (1-\nu_m^2).\left[\frac{2}{\sqrt{\pi}}\frac{1}{S_u}\sqrt{A_{cp}} - \frac{(1-\nu_i^2)}{E_i}\right]^{-1} \tag{9}$$

To determine the mechanical properties of the material investigated by instrumented indentation, one must emphasize the importance of having reliable depth values.

4 Results and discussion

Microstructural analysis of the three steels studied, who have sustained the different modes of heat treatment are shown in the metallographic figs. (2-a) and (2-b), as follows:

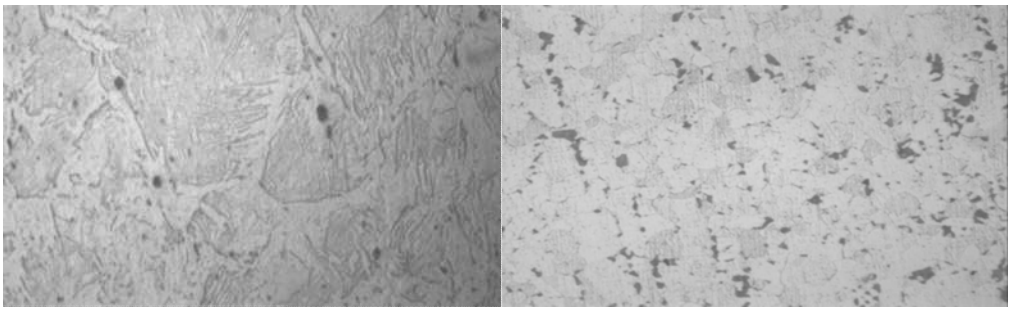

(a) (b)

Fig. 3 – Microstructure of low Carbon Steel having sustained the various heat treatments: (a) martensitic structure, (b) ferrito-perlitic structure.

Specimen No. 1: a martensitic type structure is observed in Fig.(2-a). Specimen No. 2 shows a ferrito-perlitic structure consisting of grains of more or less regular shape, see Fig.(2-b). It can be seen that the thermally affected steels have a complex multi-phase microstructure. The metallographic observation under optical microscopy allowed the observation of the martensitic and ferrito-perlitic phases in the different samples examined and thermally affected.

In the following, we try to see how instrumented indentation can help us to differentiate the mechanical properties of these different structures.

Expression of hardness [18] and depth (H, h) as a function of physical parameters (H_0, h^*):

$$\frac{H}{H_0}=\sqrt{1+\frac{h^*}{h}} \text{ ou } (\frac{H}{H_0})^2=1+\frac{h^*}{h} \tag{10}$$

H_0: True hardness.

h^*: Characterizes the dependence of the hardness with the depth of indentation; which characterizes the effect of the size and depends on the nature of the indented material, it is estimated in [nm] [19-20].

Determination of (H_0, h^*) is done by plotting the curve: H^2 as a function of 1/h according to the model of Nix and Gao; its representation is a line whose ordinate is H_0 and its slope ish^*.

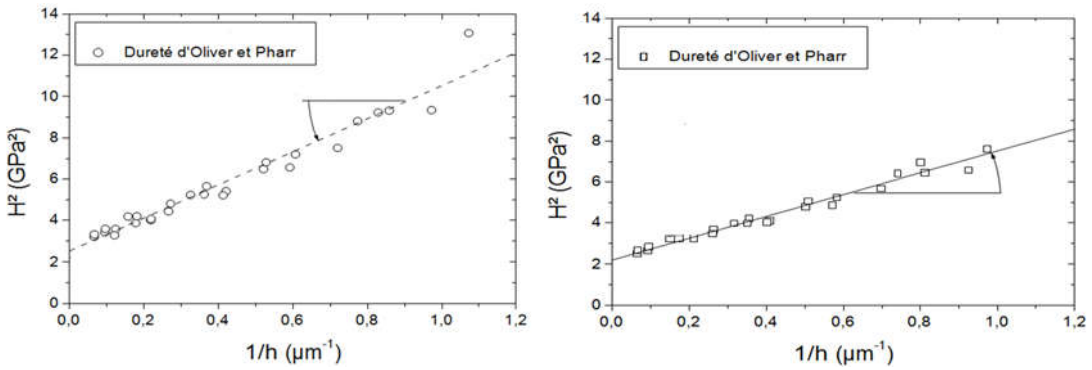

(a) (b)

Fig. 4 –Square of the hardness of Oliver and Pharr (H_{OP}) vs the inverse of the depth in a representation related to the model of Nix and Gao.

Table 1 - Values of H_M, H_{op}, h* and HLSF for each specimen tested

Parameters	Specimen a	Specimen b
H_{OP} (GPa)	1,68	1,26
h* (µm)	2,78	2,15
HLSF (MPa.m$^{1/2}$)	2,66	2,13

The calculation of the hardness, the variation of the hardness seems to follow logically what is expected for this type of treatment. Indeed, the martensitic microstructure is recognized of higher hardness than the hardness of the ferrito-perlitic steels. With respect to characteristic depth values, h*, it is not possible to show a trend because these values do not seem to follow an evolution in relation to the type of microstructure. While caution is exercised in interpreting the values of the hardness scale factor, we can note that both samples have practically the same scale factor values. This could mean that the density of dislocations involved in the deformation process is substantially the same in all cases. The plastic deformation capacity would therefore be independent of the microstructure but rather related to the material.

Using the Oliver and Pharr method, we calculated the Burgers vectors from the hardness scale factor. We have reached Burgers values of 0.90nm and 0.64nm for specimens a and b respectively.

In materials science, a dislocation is a linear defect corresponding to a discontinuity in the organization of the crystal structure. Physically, the Burgers vector represents the amplitude of the deformation carried by a dislocation. From the value of the scale factor, the Burgers vector, b, which is linked to the HLSF, and the shear modulus µ, which is 80GPa for the steel, is calculated by the relation 7 (see table. 1). The order of magnitude of the values of the Burgers vectors is coherent. In any case, all this obviously constitutes only tracks of reflection. The few results discussed here do not reveal any confirmation of these assumptions.

Calculation of the modulus of elasticity deduced from the slope of the curves; $\frac{1}{S_u}$ as a function of f ($\frac{1}{h_c}$) for the various microstructures of the steel studied.Estimate Young's modulus values for both samples a and b are 229.3GPa and 221.2GPa.

This result is surprising but interesting at the same time; the first observation we can make is that the module values found for each sample are the same as might be expected. This also confirms that the methodology is reproducible and that one can be confident of the average value found which is equal to 225.25 GPa. However, this value is far from the value of 210GPa which is found for the modulus of elasticity of steels with the conventional traction methods.

5 Conclusions

Indentation of materials is a rapidly expanding technique since the development of instrumented indentation. This is accompanied by a great deal of questioning about the reliability of the measures, all the more so as one is interested in increasingly fine scales. While advances have been made in the consideration of peak defects, deformations around the impression, indentation size effects, we still do not know how to change the scale between the domain of the microindentation and the domain of the nanoindentation. The numerous test conditions, almost infinitely, on loading and unloading speeds, maximum load holding times, constant load or increasing load cycles, also raise questions about the values of hardness or modulus of elasticity found by applying these different test conditions.

We have raised the fact that the measured module may be different from that expected by the conventional traction results. Since the latter are not always accessible to obtain the modulus of elasticity of films or coatings, alternative methods such as indentation must be used, but caution must be exercised in interpreting the results.We have demonstrated the influence of the thermal assignment on the hardness properties and the Young's modulus. We have shown that the microstructural configuration affects the local properties of low carbon steel.

We have also shown an increase in the hardness and Young's modulus with the increase of the thermal assignment. The heat treatment of a piece of metal consists in making it undergo structural transformations by means of predetermined heating and cooling cycles in order to improve the mechanical characteristics thereof: hardness, ductility, elastic limit.., etc.

REFERENCES

[1] S. Habibi, Statistical methods for the analysis of the characteristic curve of brass by Vickers indentation. Mechanika. Vol. 22(6) (2016) pp. 478-482.
[2] L. Aminallah, S. Habibi, Exploitation of Nanoindentation and Statistical Tools to Investigate the Behavior of Materials. Eng Technol Appl Sci Res. Vol. 6(4) (2016) pp. 1089-1092.
[3] D. Zebbar, S. Zebbar, S. Horr, Étude théorique du principe de construction des structures des bilans énergétiques interne et externe d'un moteur diesel. Recueil de mécanique, centre universitaire de Tissemsilt. Vol. 1 (2016) pp. 041-048.
[4] S. Kossman, D. Chicot et A. Iost, Indentation instrumentée multi-échelles appliquée à l'étude des matériaux massifs métalliques. Journal de Matériaux et Techniques. Vol. 105 (1) (2017).
[5] Y.T. Cheng, C.M.Cheng, Scaling, dimensional analysis, and indentation measurements. Mater Sci Eng R. Vol. 44 (2004) 91-149.
[6] D. Chicot, D. Mercier, Improvement in depth-sensing indentation to calculate the universal hardness on the entire loading curve. Mech Mater. Vol. 40 (2008) pp.171-182.
[7] O. Sahin, O. Uzun, U. Kolemen and N. Uçar, Analysis of ISE in dynamic hardness measurements of β-Sn single crystals using a depth-sensing indentation technique. Mater Charact. Vol. 59 (2008) pp.729-736.
[8] D.Chicot, F.Roudet, V.Lepingle, G.Louis, Strain gradient plasticity to study hardness behaviour of magnetite (FE3O4) under multicyclic indentation. J Mater Res., 24 (3) (2009) pp. 749-759.
[9] J.M. Antunes, J.V. Fernandes, L.F. Menezes, B.M. Chaparro, A new approach for reverse analyses in depth-sensing indentation using numerical simulation. Acta Mater.Vol.55(2013) pp.69-81.
[10] D. Chicot, P. de Baets, MH. Staia, ES. Puchi-Cabrera, G. Louis, Y. Perez Delgado. Influence of tip defect and indenter shape on the mechanical properties determination by indentation of a TiB2–60% B4C ceramic composite. Inter J Refract Met Hard Mater. Vol. 38 (2013) pp.102–10.
[11] W.C. Oliver and G.M. Pharr, An Improved Technique for Determining Hardness and Elastic Modulus using Load and Displacement Sensing Indentation measurements. Journal of Materials Research. Vol. 7 (1992) pp.1564-1583.
[12] M.R. Van Landingham, Review of instrumented indentation, J Res Nat Inst Stand Techn. Vol. 108 (2003) pp. 249-265.
[13] G.M Pharr, A. Bolshakov, Understanding nanoindentation unloading curves. J Mater Res. Vol. 17 (10)(2002) pp. 2660-2671.
[14] O.Uzun, U.Kolemen, S.Çelebi, N.Guclu, Modulus and hardeness evaluation of polycrystalline superconductors by dynamic microindentation technique. J Eur Ceram Soc., 25, 26 (2005) pp. 969-977.
[15] H.Hertz, On the contact of elastic solids. Miscellaneous Papers, Macmillan, London Chapter 5, (1896) pp. 146-183.
[16] S.I.Bulychev, V.P.Alekhin, M.K.Shorshorov, A.P.Ternovskii, G.D.Shnyrev, Determining Young's modulus from the indentor penetration diagram. ZavodLab., 39(1973) pp. 1137-1142.
[17] I.N.Sneddon, The relationship between load penetration in the axisymmetric Boussinesq problem for a punch of arbitrary profile. Int J Eng Sci., 3 (1965) pp. 47-57.
[18] P.J. Blau, A comparison of four microindentation hardness test methods using copper, 52100 steel, and an amorphous Pd-Cu-Si alloy. Metall. 16 (1983) pp. 1-18.
[19] D.B Marshall, B.R. Lawn, Microindentation Techniques in Matérials Science and Engineering. ASTM, Philadelphia, PA, (1986)26.
[19] S.J Bull, T.F. Page, E.H. Yoffe, An explanation of the indentation size effect in ceramics. Phil Mag Lett. Vol. 59 (1989) pp. 281-288.